Graphene electrostatic microphone and ultrasonic radio

Qin Zhou (周勤)[a,b,c], Jinglin Zheng[a], Seita Onishi[a,b,c], M. F. Crommie[a,b,c], and Alex K. Zettl[a,b,c,1]

[a]Department of Physics, University of California, Berkeley, CA 94720; [b]Materials Sciences Division, Lawrence Berkeley National Laboratory, Berkeley, CA 94720; and [c]Kavli Energy NanoSciences Institute at the University of California and the Lawrence Berkeley National Laboratory, Berkeley, CA 94720

Edited by Donhee Ham, Harvard University, Cambridge, MA, and accepted by the Editorial Board June 1, 2015 (received for review March 24, 2015)

We present a graphene-based wideband microphone and a related ultrasonic radio that can be used for wireless communication. It is shown that graphene-based acoustic transmitters and receivers have a wide bandwidth, from the audible region (20∼20 kHz) to the ultrasonic region (20 kHz to at least 0.5 MHz). Using the graphene-based components, we demonstrate efficient high-fidelity information transmission using an ultrasonic band centered at 0.3 MHz. The graphene-based microphone is also shown to be capable of directly receiving ultrasound signals generated by bats in the field, and the ultrasonic radio, coupled to electromagnetic (EM) radio, is shown to function as a high-accuracy rangefinder. The ultrasonic radio could serve as a useful addition to wireless communication technology where the propagation of EM waves is difficult.

radio | ultrasonics | graphene | microphone | bat

Modern wireless communication is based on generating and receiving electromagnetic (EM) waves that span a wide frequency range, from hertz to terahertz, providing abundant band resources and high data transfer rates. There are drawbacks to EM communication, though, including high extinction coefficient for electrically conductive materials and antenna size. However, animals have effectively used acoustic waves for short-range communication for millions of years. Acoustic wave-based communication, while embodying reduced band resources, can overcome some of the EM difficulties and complement existing wireless technologies. For example, acoustic waves propagate well in conductive materials, and have thus been explored for underwater communication by submarines (1, 2). Marine mammals such as whales and dolphins are known to communicate effectively via acoustic waves. In land-based acoustic wave communication, the audible band is often occupied by human conversations, whereas the subsonic band can be disturbed by moving vehicles and building construction. The ultrasonic band, though having a wide frequency span and often free of disturbance, is rarely exploited for high data rate communication purposes; one possible reason for this is the lack of wide bandwidth ultrasonic generators and receivers. Conventional piezoelectric-based transducers only operate near their resonance frequencies (3, 4), preventing use in communications where wider bandwidth is essential for embedding information streams.

In a conventional acoustic transducer such as a microphone, air pressure variations from a sound wave induce motion of a suspended diaphragm; this motion is in turn converted to an electrical signal via Faraday induction (using a magnet and coil) or capacitively. The areal mass density of the diaphragm sets an upper limit on the frequency response (FR) of the microphone. In the human auditory system, the diaphragm (eardrum) is relatively thick (∼100 μm), limiting flat FR to ∼2 kHz and ultimate detection to ∼20 kHz (5, 6). In bats the eardrums are thinner, allowing them to hear reflected echolocation calls up to ∼200 kHz (7–9). Diaphragms in high-end commercial microphones can be engineered to provide flat FR from the audible region to ∼140 kHz (e.g., Bruel & Kjaer type 4138 microphone). Thinner and lighter diaphragms allow for more faithful tracking of sound vibration at high frequencies.

The ultra-low mass and high mechanical strength of graphene makes it extremely attractive for sound transduction applications (10). We have previously demonstrated an electrostatically driven graphene diaphragm loudspeaker with an equalized FR across the whole human audible region (11) (20 Hz to 20 kHz). The ultimate high-frequency cutoff of the speaker was not determined, the measurement being limited to 20 kHz by available detection equipment (indeed, as shown below, the graphene loudspeaker operates to at least 0.5 MHz). Graphene allows air damping to dominate over the diaphragm's own mass and spring constant (11) over a wide frequency range. In principle, graphene's exceptional mechanical properties and favorable coupling to air and other media could enable wideband transducers for both sound generation and reception, core requirements for ultrasonic radio.

We here describe the successful design, construction, and operation of a wideband ultrasonic radio. A key ingredient of the radio system is an electrostatically coupled, mechanically vibrating graphene diaphragm based receiver that can be paired with the graphene-based acoustic transmitter. We find that the graphene microphone has an outstanding equalized frequency response (within 10 dB variation of perfect flat-band response) covering at least 20 Hz to 0.5 MHz (limited by characterization instrumentation), and a sensitivity sufficient to record bats echolocating in the wild. The highly efficient graphene ultrasonic transmitter/receiver radio system successfully codes, propagates, and decodes radio signals. The same radio system can be used to

Significance

Humans and other animals effectively use acoustic waves to communicate with each other. Ultrasonic acoustic waves are intriguing because they do not interfere with normal voice communication and can be highly directional with long range. Therefore, wireless ultrasonic radio is a useful communications method. Here we find that graphene has mechanical properties that make it ideally suited for wide-band ultrasonic transduction. Using simple and low-cost fabrication methods we have produced an ultrasonic microphone and ultrasonic radio prototypes. When acting as loudspeaker/microphone alone, the graphene-based acoustic devices also show ideal flat-band frequency response spanning the whole audible region as well as ultrasonic region to at least 0.5 MHz; such flat frequency response has significant acoustic applications implications.

Author contributions: Q.Z., J.Z., and A.K.Z. designed research; Q.Z., J.Z., S.O., and A.K.Z. performed research; M.F.C. and A.K.Z. contributed new reagents/analytic tools; Q.Z. and A.K.Z. analyzed data; and Q.Z. and A.K.Z. wrote the paper.

The authors declare no conflict of interest.

This article is a PNAS Direct Submission. D.H. is a guest editor invited by the Editorial Board.

[1]To whom correspondence should be addressed. Email: azettl@berkeley.edu.

This article contains supporting information online at www.pnas.org/lookup/suppl/doi:10.1073/pnas.1505800112/-/DCSupplemental.

accurately measure distances using interference between ultrasonic and electromagnetic waves.

We first describe construction and operation of the graphene microphone, followed by operation of the ultrasonic radio and rangefinder. Fig. 1 illustrates the geometry and construction of the graphene receiver. Briefly, the microphone is built from a multilayer graphene membrane (~20 nm thick, 7 mm in diameter) suspended midway between two perforated electrodes. The external sound wave can then penetrate through the electrodes to displace the graphene membrane, thereby changing the capacitance between the graphene and electrodes and causing charge redistribution and electrical current. The geometry is motivated by the graphene electrostatic loudspeaker (11), with an improved fabrication process described in *SI Text*. Fig. 1 *D* and *E* illustrates the operation principles of the microphone and presents competing circuits for signal extraction. Conventionally (12) (Fig. 1*D*), a large resistor R restricts the current flow and lets the diaphragm operate in constant charge mode, which converts the displacement of the diaphragm into voltage signal (a related circuit is presented in reference) (13). However, this circuit presents difficulties at higher frequencies because of parasitic capacitance present in the electrical wiring between the microphone and amplifier. We adopt a transimpedance amplification circuit similar to one used in fast photodiode signal detection (14) (Fig. 1*E*) to provide a flat band circuit response from 0 to ~0.5 MHz. The current sensing circuit measures the velocity of the vibrating diaphragm, allowing us to reduce the membrane tension and operate the microphone in overdamped region to acquire wider frequency response (see *SI Text* for detailed operation theory).

To determine the frequency response of the graphene microphone, we measured the microphone using a free-field method (15). In brief, we first sweep the frequency on a commercial loudspeaker and measure the response of a commercial microphone to obtain the frequency response $FR_1(f)$, then the commercial microphone is replaced with the graphene microphone and the measurement is repeated to get $FR_2(f)$. The FR of the graphene microphone is acquired by taking the difference between the two measurements. This differential measurement method eliminates the responses of the loudspeaker, coupling, and driving/amplification circuits. Commercial microphones typically have a relatively flat frequency response within their operating range, and therefore this measurement provides a reasonable representation of the graphene microphone.

Fig. 2*A* shows the frequency response of the graphene microphone in the audible region (20 Hz to 20 kHz), referenced to a commercial condenser microphone (Sony ICD-SX700). Here, 0 dB corresponds to a response of 3.3 nA/Pa generated from the graphene membrane. A computer sound card-based system with software Room EQ Wizard is used in collecting the data. The graphene microphone is contained in a Faraday cage made of copper mesh. Although in Fig. 2*A* the data are relatively flat above 500 Hz, there is a strong drop-off in response at lower frequencies (approaching ~60 dB per decade). This drop-off originates from the back-to-front cancelation mentioned previously, and becomes prominent when increasing wavelength allows sound to diffract around the microphone. Importantly, this decay is not intrinsic to the graphene diaphragm itself, and the response can be improved with proper acoustic design. We find that an improved low-frequency response can readily be achieved by attaching an acoustic cavity to one side of the microphone electrodes. As shown in Fig. 2*B*, by simple acoustic engineering we eliminate low-frequency interference and the graphene microphone now exhibits an intrinsic flat (<10 dB variation) frequency response across the whole audible region.

Due to the small areal mass density of the thin graphene diaphragm, the graphene microphone is expected to be responsive to frequencies well beyond the human hearing limit. However,

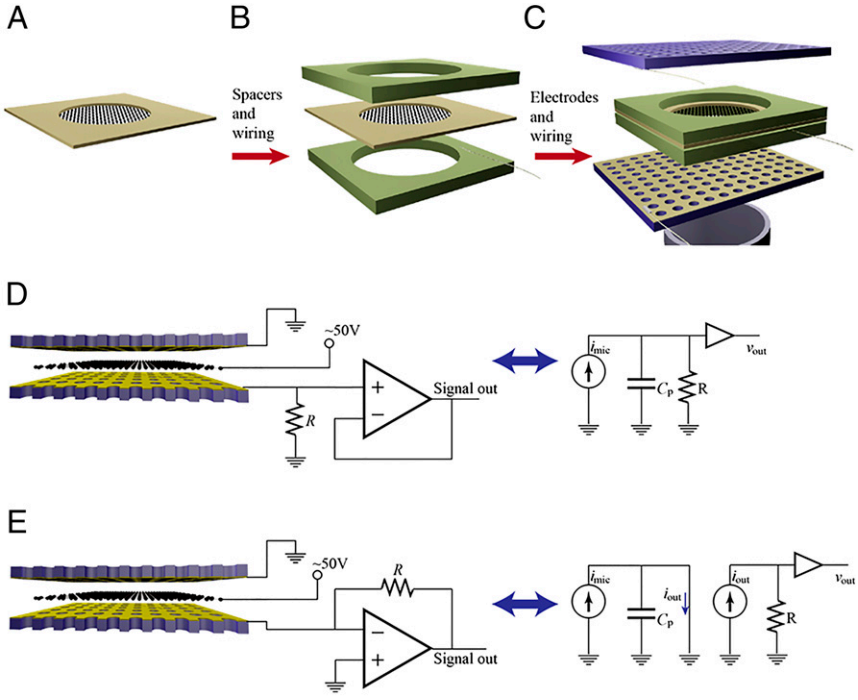

Fig. 1. Construction of graphene electrostatic wideband receiver (microphone). The graphene membrane is suspended across the supporting frame (*A*). The membrane is electrically contacted with gold wires, and spacers are added (*B*) to control the distance from the membrane to the gold-coated stationary electrodes (*C*). Operation principles: the microphone can be modeled as a current source i_{mic}. The conventional circuit (*D*) is not suitable for high-frequency operation because parasitic capacitance C_p is in parallel with the current–voltage conversion resistor R. The fast-photodiode detector-like circuit (*E*) avoids charging C_p and maintains a consistent gain at higher frequencies.

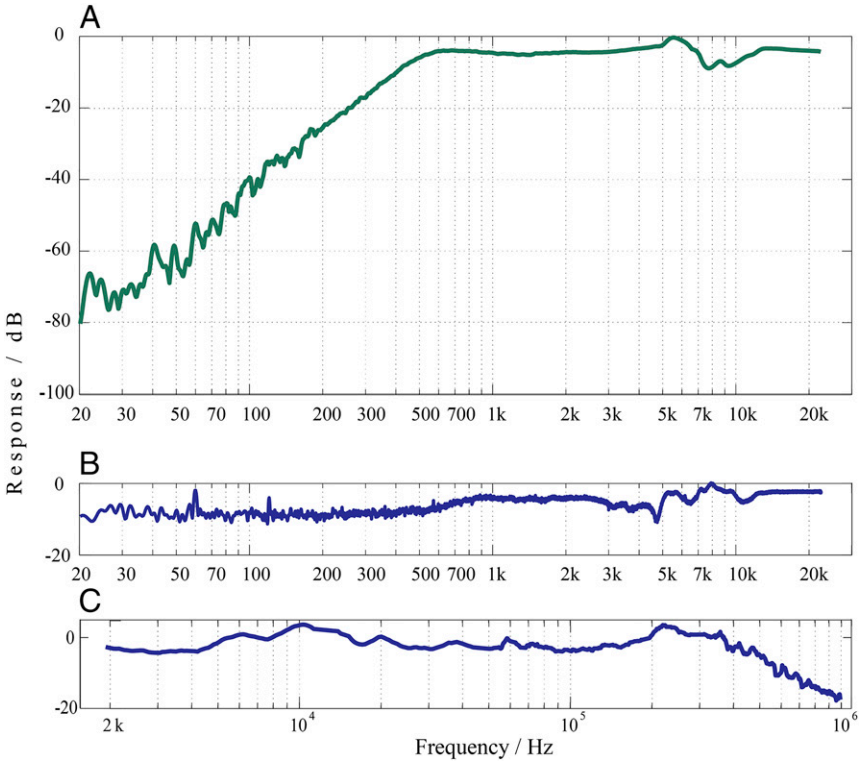

Fig. 2. Measured frequency response of graphene acoustic transmitter and receiver. *A* and *B* are measured in reference to Sony ICD-SX700 in audible region. Zero decibels corresponds to a response of 3.3 nA/Pa. (*A*) Without an acoustic cavity, the frequency response suffers from interference at lower frequencies when measuring far-field sound waves. (*B*) Graphene microphone exhibits rather equalized frequency response with near-field coupling and proper acoustic design. (*C*) Response including ultrasonic region, measured with identical pair technique (main text and *SI Text*). The response fall-off beyond 0.5M Hz is not intrinsic to the acoustic device, but rather reflects limitations of the operational amplifier used in the detection circuit.

measuring the frequency response in the ultrasonic region presents difficulties, mainly due to the lack of wideband reference microphones or loudspeakers in this region. As mentioned, piezoelectric ultrasonic transducers readily operate in the megahertz region, but only at their resonance frequency. We therefore use a wideband electrostatic graphene loudspeaker as the sonic transmitter and the electrostatic graphene microphone as the receiver. By measuring the total response with varying coupling between them, we are able to isolate the response of one single transmitter/receiver (see *SI Text* for details).

Fig. 2*C* illustrates the measured frequency response of the graphene microphone (a network analyzer, model HP3577A, is used for the measurement because the frequencies exceed the limits of a conventional computer sound card). The response appears to be relatively flat (within 10 dB) until ∼0.5 MHz. We note that the measured maximum frequency of flat FR is only limited by the electronic amplification circuit, and can be extended using higher bandwidth operational amplifiers or with different detection methods such as optical detection (16, 17). Combining this result with the low-frequency measurements (Fig. 2*B*), we conclude that the graphene transmitter/receiver pair has intrinsic equalized frequency response (with variation less than 10 dB) from 20 Hz to at least 0.5 MHz, ideal for ultrasonic radio operation.

As an initial ultrasonic field test of the graphene receiver, we record ultrasonic bat calls. Bats often use echolocation to navigate and forage in total darkness. Bat call frequencies range from as low as 11 kHz to as high as 212 kHz, depending on the species (8, 9). Fig. 3*A* shows results from ultrasonic bat sound signals (bat calls) acquired in the field using the graphene electrostatic microphone at Del Valle Regional Park, Livermore, CA, where the bat species western pipistrelle (*Parastrellus hesperus*) is prevalent. The spectrogram of Fig. 3*A* shows that these bat calls consist of periodic chirps during which the emitted frequency consistently ramps down in frequency from ∼100 kHz to ∼50 kHz. The duration of each chirp is ∼4 ms, and the repeating period is ∼50 ms. It is believed that bats use the frequency-sweeping technique to distinguish multiple targets, improve measurement accuracy, and avoid interference from each other (8, 18, 19). A direct recording (amplitude vs. time) of the bat calls is included in *SI Text* (slowed by a factor of 8 to bring the signal into the human hearing range). The bat frequency sweeping or chirping represents a form of ultrasonic FM radio transmission, and its successful recording demonstrates the effectiveness of the graphene microphone as an ultrasonic radio receiver.

We now pair the ultrasonic graphene transmitter with the ultrasonic graphene receiver to realize a complete ultrasonic radio system. To avoid any possible EM radiation influences, both the transmitter and the receiver are placed inside Faraday cages where EM communication is not possible. We first modulate an electronic 0.3-MHz carrier sine wave with a 5-kHz sawtooth wave [90% amplitude modulation (AM)]. The mixed signal is monitored by an oscilloscope (Fig. 3*B*, *Upper*). The electrical signal is sent to the graphene loudspeaker, which transmits the ultrasonic signal into air. The frequencies after mixing are well above the human hearing limit and so inaudible. Fig. 3*B*, *Lower*, shows the ultrasonic signal detected and reconverted to an electrical signal by the graphene microphone. The received signal accurately replicates the transmitted one, and information is transmitted with high fidelity. We note that the sharp sawtooth modulation expands the single delta-function-like peak of the sine wave in the frequency domain to a much wider peak, so the wideband property of the graphene acoustic radio is essential to preserve the shape of the sawtooth (i.e., coded information). Narrowband piezoelectric

ultrasonic transducers lack this essential property (*SI Text*). The range of the ultrasonic radio as configured with single-diaphragm transmitter and single-diaphragm receiver is of order one meter. The range can likely be substantially extended by employing diaphragm arrays and optimized drive/detection electronics.

Another use of the graphene-based ultrasonic acoustic radio is for position detection, i.e., range finding. Using ultrasonics for position detection is well established, and using the graphene transmitter and receiver in a highly directional sonar-like reflection configuration (20) is certainly possible and straightforward, but not particularly novel. Here we consider a different implementation, that of electroacoustic interference. Fig. 3*C* illustrates a distance-measuring device that exploits interference between acoustic and EM signals. The graphene loudspeaker is configured to transmit an acoustic wave as well as an EM wave of the same frequency (a small EM antenna is added to the loudspeaker drive electronics). The graphene microphone a distance L away receives the acoustic signal along with the EM signal (again a small EM receiver

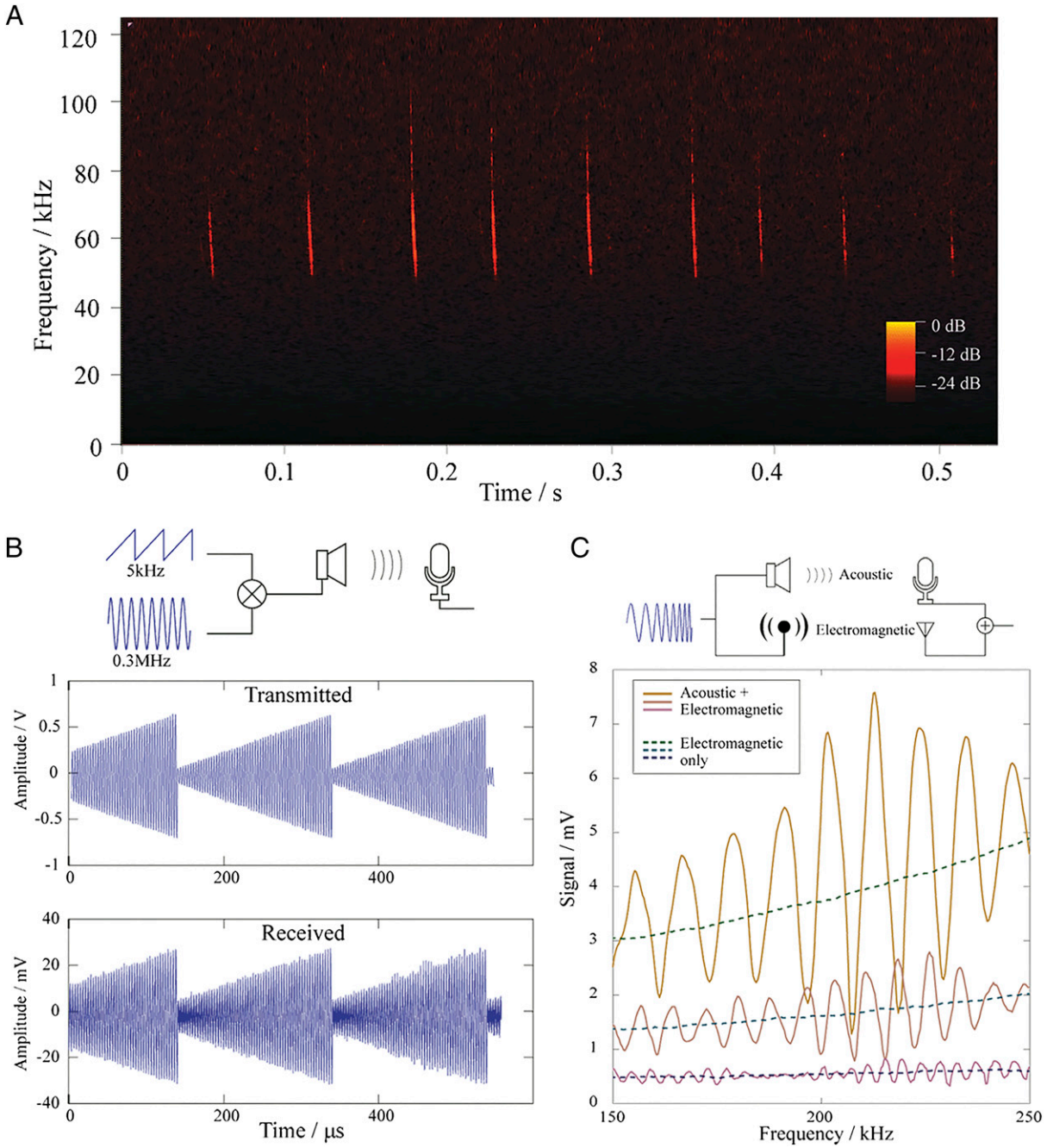

Fig. 3. Applications of wideband ultrasonic graphene acoustic transducers. (*A*) Spectrogram of bat calls (*Parastrellus hesperus*) recorded in the field at a local park. During each 4-ms-wide emission chirp, the frequency ramps down from ~100 to ~50 kHz. The time between chirps ranges from 30 to 50 ms. (*B*) The transmission and reception of AM acoustic signals. The wideband acoustic radio well-preserves the sharp edges of the sawtooth envelope. (*C*) A way of measuring distance by frequency sweeping. The oscillation comes from the interference between the signals picked up from acoustic waves and electromagnetic waves, and the distance between the speaker and microphone is derived to be equal to the speed of sound divided by the pitch between the peaks.

antenna is added to the transducer electronics on the microphone). Because sound propagates much slower than EM waves, the sound signal picked up by the microphone diaphragm will develop a phase difference relative to the EM signal of the electronic receiver antenna. As readily seen in Fig. 3*C*, when a frequency sweep is performed, the interference alternates between constructive and destructive due to the change in the wavelength λ. We place the graphene speaker/microphone pair three different distances apart, at 30, 45, and 85 mm. The measured frequency sweep is shown from top to bottom in three groups in Fig. 3*C*. When the pair is further apart, the signal is weaker, and the frequency difference between two constructive peaks also becomes smaller; by fitting in the data (*SI Text*) and using a sound velocity of 344 m/s, this corresponds to a measured distance of 30.49 ± 0.22 mm, 44.92 ± 0.02 mm, and 84.94 ± 0.84 mm (the uncertainty comes from curve fitting). Submillimeter accuracy is easily achieved with this simple electroacoustic frequency sweep configuration.

In conclusion, an electrostatic graphene acoustic radio is demonstrated with ideal equalized frequency response from at least 20 Hz to 0.5 MHz. The receiver component has been independently field-tested in recording wild bat calls. Amplitude- and frequency-modulated communication is demonstrated, and an electroacoustic range-finding method is established with the ultrasonic radio having submillimeter accuracy.

ACKNOWLEDGMENTS. This work was supported in part by the Director, Office of Energy Research, Office of Basic Energy Sciences, Materials Sciences and Engineering Division, US Department of Energy Contract DE-AC02-05CH11231, which provided for graphene growth and characterization; Office of Naval Research Grant N00014-09-1066, which provided for graphene transfer and electrode manufacture; and by National Science Foundation Grant EEC-083819, which provided for design, construction, and testing of the device.

1. Kilfoyle DB, Baggeroer AB (2000) The state of the art in underwater acoustic telemetry. *IEEE J Oceanic Eng* 25(1):4–27.
2. Proakis JG, ed (2003) *Wiley Encyclopedia of Telecommunications* (Wiley, Hoboken, NJ).
3. Gururaja TR, et al. (1985) Piezoelectric composite materials for ultrasonic transducer applications. Part I: Resonant modes of vibration of PZT rod-polymer composites. *IEEE Trans Sonics Ultrason* 32(4):481–498.
4. Gómez Alvarez-Arenas TE (2004) Acoustic impedance matching of piezoelectric transducers to the air. *IEEE Trans Ultrason Ferroelectr Freq Control* 51(5):624–633.
5. Sun Q, Gan RZ, Chang K-H, Dormer KJ (2002) Computer-integrated finite element modeling of human middle ear. *Biomech Model Mechanobiol* 1(2):109–122.
6. Prendergast PJ, Ferris P, Rice HJ, Blayney AW (1999) Vibro-acoustic modelling of the outer and middle ear using the finite-element method. *Audiol Neurootol* 4(3-4): 185–191.
7. Hill JE, Smith JD (1984) *Bats: A Natural History* (Univ of Texas Press, Austin, TX).
8. Jones G, Holderied MW (2007) Bat echolocation calls: Adaptation and convergent evolution. *Proc Biol Sci* 274(1612):905–912.
9. Fenton M, Bell G (1981) Recognition of species of insectivorous bats by their echolocation calls. *J Mammal* 62(2):233–243.
10. Lee C, Wei X, Kysar JW, Hone J (2008) Measurement of the elastic properties and intrinsic strength of monolayer graphene. *Science* 321(5887):385–388.
11. Zhou Q, Zettl A (2013) Electrostatic graphene loudspeaker. *Appl Phys Lett* 102(22): 223109.
12. Eargle J (2005) *The Microphone Book* (Focal Press, Oxford).
13. Choi HS, Hur S, Lee YH (2012) World Intellectual Property Organization Patent Appl WO2011142637A2 (February 2, 2012).
14. Horowitz P, Hill W (1989) *The Art of Electronics* (Cambridge Univ Press, Cambridge, UK).
15. Zuckerwar A (2006) Calibration of the pressure sensitivity of microphones by a free-field method at frequencies up to 80 kHz. *J Acoust Soc Am* 119(1):320–329.
16. Bunch JS, et al. (2007) Electromechanical resonators from graphene sheets. *Science* 315(5811):490–493.
17. Barton RA, et al. (2011) High, size-dependent quality factor in an array of graphene mechanical resonators. *Nano Lett* 11(3):1232–1236.
18. Jones G, Teeling EC (2006) The evolution of echolocation in bats. *Trends Ecol Evol* 21(3):149–156.
19. Fenton MB, Portfors CV, Rautenbach IL, Waterman JM (1998) Compromises: Sound frequencies used in echolocation by aerial-feeding bats. *Can J Zool* 76:1174–1182.
20. Kay L (1964) An ultrasonic sensing probe as a mobility aid for the blind. *Ultrasonics* 2(2):53–59.
21. Temkin S (1981) *Elements of Acoustics* (Wiley, New York).
22. Tay RY, et al. (2014) Growth of large single-crystalline two-dimensional boron nitride hexagons on electropolished copper. *Nano Lett* 14(2):839–846.
23. Wensch G (1950) Electrolytic polishing of nickel. *Met Prog* 58:735–736.
24. Tsen AW, et al. (2012) Tailoring electrical transport across grain boundaries in polycrystalline graphene. *Science* 336(6085):1143–1146.
25. Kim KS, et al. (2009) Large-scale pattern growth of graphene films for stretchable transparent electrodes. *Nature* 457(7230):706–710.
26. Alemán B, et al. (2013) Polymer-free, low tension graphene mechanical resonators. *Phys Status Solidi Rapid Res Lett* 7(12):1064–1066.
27. Weaver W, Timoshenko SP, Young DH (1990) *Vibration Problems in Engineering* (Wiley, New York), 5th Ed.